



# Geochemical provenancing and direct dating of the Harbin archaic human cranium

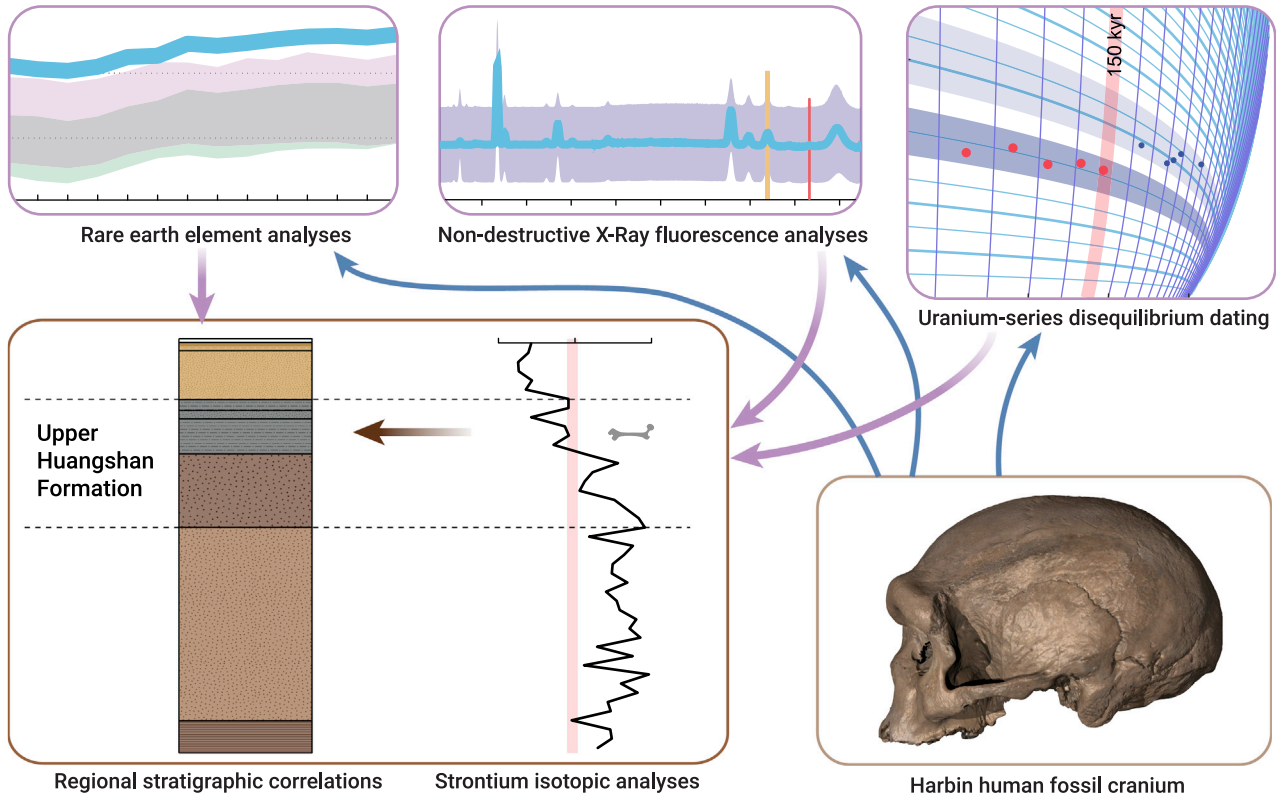
Qingfeng Shao,<sup>1,12</sup> Junyi Ge,<sup>2,3,12</sup> Qiang Ji,<sup>4,\*</sup> Jinhua Li,<sup>5</sup> Wensheng Wu,<sup>4</sup> Yannan Ji,<sup>6</sup> Tao Zhan,<sup>7</sup> Chi Zhang,<sup>2,3</sup> Qiang Li,<sup>2,3</sup> Rainer Grün,<sup>8,9,\*</sup> Chris Stringer,<sup>10,\*</sup> and Xijun Ni<sup>2,3,4,11,\*</sup>

\*Correspondence: [nixijun@hgu.edu.cn](mailto:nixijun@hgu.edu.cn) (X.N.); [jqiang@hgu.edu.cn](mailto:jqiang@hgu.edu.cn) (Q.J.); [rainer.grun@griffith.edu.au](mailto:rainer.grun@griffith.edu.au) (R.G.); [c.stringer@nhm.ac.uk](mailto:c.stringer@nhm.ac.uk) (C.S.)

Received: May 10, 2021; Accepted: June 4, 2021; Published Online: June 25, 2021; <https://doi.org/10.1016/j.xinn.2021.100131>

© 2021 The Author(s). This is an open access article under the CC BY-NC-ND license (<http://creativecommons.org/licenses/by-nc-nd/4.0/>).

## Graphical abstract



## Public summary

- Unsystematic recovery of the Harbin fossil cranium and a long history since the discovery impede its accurate dating
- Geochemical analyses, including non-destructive X-ray fluorescence, rare earth elements, and the strontium isotopes, suggest that the fossil cranium was from a bed of lacustrine sediments aged between 138 and 309 thousand years ago in the Harbin region
- Uranium-series disequilibrium dating directly on the cranium suggests that the cranium is older than 146 thousand years



# Geochemical provenancing and direct dating of the Harbin archaic human cranium

Qingfeng Shao,<sup>1,12</sup> Junyi Ge,<sup>2,3,12</sup> Qiang Ji,<sup>4,\*</sup> Jinhua Li,<sup>5</sup> Wensheng Wu,<sup>4</sup> Yannan Ji,<sup>6</sup> Tao Zhan,<sup>7</sup> Chi Zhang,<sup>2,3</sup> Qiang Li,<sup>2,3</sup> Rainer Grün,<sup>8,9,\*</sup> Chris Stringer,<sup>10,\*</sup> and Xijun Ni<sup>2,3,4,11,\*</sup>

<sup>1</sup>Key Laboratory of Virtual Geographic Environment, Ministry of Education, Nanjing Normal University, Nanjing 210023, China

<sup>2</sup>CAS Center for Excellence in Life and Paleoenvironment, Chinese Academy of Science, Beijing 100044, China

<sup>3</sup>University of Chinese Academy of Sciences, Beijing 100049, China

<sup>4</sup>Hebei GEO University, Shijiazhuang 050031, China

<sup>5</sup>Key Laboratory of Earth and Planetary Physics, Innovation Academy for Earth Science, Chinese Academy of Sciences, Beijing 100029, China

<sup>6</sup>China Geo-Environmental Monitoring Institute, Beijing 100081, China

<sup>7</sup>The Second Hydrogeology and Engineering Geology Prospecting Institute of Heilongjiang Province, Harbin 150030, China

<sup>8</sup>Australian Research Centre for Human Evolution, Griffith University, Nathan, QLD, Australia

<sup>9</sup>Research School of Earth Sciences, The Australian National University, Canberra, ACT, Australia

<sup>10</sup>Centre for Human Evolution Research, Department of Earth Sciences, Natural History Museum, London, UK

<sup>11</sup>CAS Center for Excellence in Tibetan Plateau Earth Sciences, Chinese Academy of Science, Beijing 100104, China

<sup>12</sup>These authors contributed equally

\*Correspondence: nixijun@hgu.edu.cn (X.N.); jiqiang@hgu.edu.cn (Q.J.); rainer.grun@griffith.edu.au (R.G.); c.stringer@nhm.ac.uk (C.S.)

Received: May 10, 2021; Accepted: June 4, 2021; Published Online: June 25, 2021; <https://doi.org/10.1016/j.xinn.2021.100131>

© 2021 The Author(s). This is an open access article under the CC BY-NC-ND license (<http://creativecommons.org/licenses/by-nc-nd/4.0/>).

Citation: Shao Q., Ge J., Ji Q., et al., (2021). Geochemical provenancing and direct dating of the Harbin archaic human cranium. *The Innovation* 2(3), 100131.

As one of the most complete archaic human fossils, the Harbin cranium provides critical evidence for studying the diversification of the *Homo* genus and the origin of *Homo sapiens*. However, the unsystematic recovery of this cranium and a long and confused history since the discovery impede its accurate dating. Here, we carried out a series of geochemical analyses, including non-destructive X-ray fluorescence (XRF), rare earth elements (REE), and the Sr isotopes, to test the reported provenance of the Harbin cranium and get better stratigraphic constraints. The results show that the Harbin cranium has very similar XRF element distribution patterns, REE concentration patterns, and Sr isotopic compositions to those of the Middle Pleistocene-Holocene mammalian and human fossils recently recovered from the Harbin area. The sediments adhered in the nasal cavity of the Harbin cranium have a  $^{87}\text{Sr}/^{86}\text{Sr}$  ratio of 0.711898, falling in the variation range measured in a core drilled near the Dongjiang Bridge, where the cranium was discovered during its reconstruction. The regional stratigraphic correlations indicate that the Harbin cranium was probably from the upper part of the Upper Huangshan Formation of the Harbin area, which has an optically stimulated luminescence dating constraint between 138 and 309 ka. U-series disequilibrium dating ( $n = 10$ ) directly on the cranium suggests that the cranium is older than 146 ka. The multiple lines of evidence from our experiments consistently support the theory that the Harbin cranium is from the late Middle Pleistocene of the Harbin area. Our study also shows that geochemical approaches can provide reliable evidence for locating and dating unsystematically recovered human fossils, and potentially can be applied to other human fossils without clear provenance and stratigraphy records.

**Keywords:** human fossil provenancing; non-destructive X-ray fluorescence; rare earth elements; strontium (Sr) isotopic composition; uranium-series disequilibrium (U-series) dating

## INTRODUCTION

The Middle Pleistocene Harbin human cranium (HBSM2018-000018(A)) is one of the best-preserved of all archaic human fossils, and has great significance for understanding the diversification of the *Homo* genus and the origin of *Homo sapiens*.<sup>1</sup> It represents a new human lineage evolving in East Asia, and is placed as a member of the sister group of *H. sapiens*.<sup>1</sup> A combination of primitive and derived features in the Harbin cranium establishes a good set

of diagnostic features that were used to define a new *Homo* species.<sup>2</sup> The Harbin cranium was reportedly discovered in 1933 during construction work when a bridge (Dongjiang Bridge) was built over the Songhua River in Harbin City in Northeastern China<sup>3</sup> (Figure 1). Because of a long, difficult, and confused history since the discovery, the information about the exact geographic origin and stratigraphical context of the cranium has been lost, impeding its accurate dating.<sup>1</sup> Here, we tested the concentrations of rare earth elements (REEs) and the Sr isotopic composition of the human fossil, and a range of mammalian fossils collected from deposits of the Songhua River near the supposed locality (Dongjiang Bridge), and used non-destructive X-ray fluorescence (XRF) analyses to examine the element distributions of these human and mammalian fossils. We also directly dated the Harbin fossil cranium by the uranium-series disequilibrium (U-series) method. The results of these analyses provided consistent evidence for the theory that the Harbin cranium is from the late Middle Pleistocene of the Harbin area.

## RESULTS

### Non-destructive XRF analyses

The non-destructive XRF analyses were conducted on the Harbin cranium and a range of mammalian fossils collected from the Pleistocene deposits of the Songhua River in Harbin area, Jiangsu Province and Guangxi Province. All the tested samples, including the two control rhinoceros fossils, have a similar XRF pattern in terms of major elements, such as Ca, P, Fe, and Mn, with various concentrations among different samples. The XRF pattern for minor elements, such as Sr, Y, and Zr are obviously different between the tested samples and the control samples (Figure 2A). Zr is undetectable from the two control samples. The Harbin cranium and the mammalian fossils from the Harbin area show almost identical XRF patterns in term of the relative amount of Sr, Y, and Zr (Figure 2A). The XRF analyses support that the Harbin cranium and the collected Harbin mammalian fossils were probably buried and fossilized in the same environment.

### REE concentration pattern

The REE concentration pattern has been proved to be an effective tool for tracing the origins of the fossils and living creatures.<sup>7–10</sup> Small bone pieces from the nasal cavity of the Harbin cranium were carefully collected for REE analyses. For comparison, fossil fragments from seven mammals and two human individuals recovered from the deposits of the Songhua River in the Harbin area were also analyzed (Figures S1 and S2). The ages of these

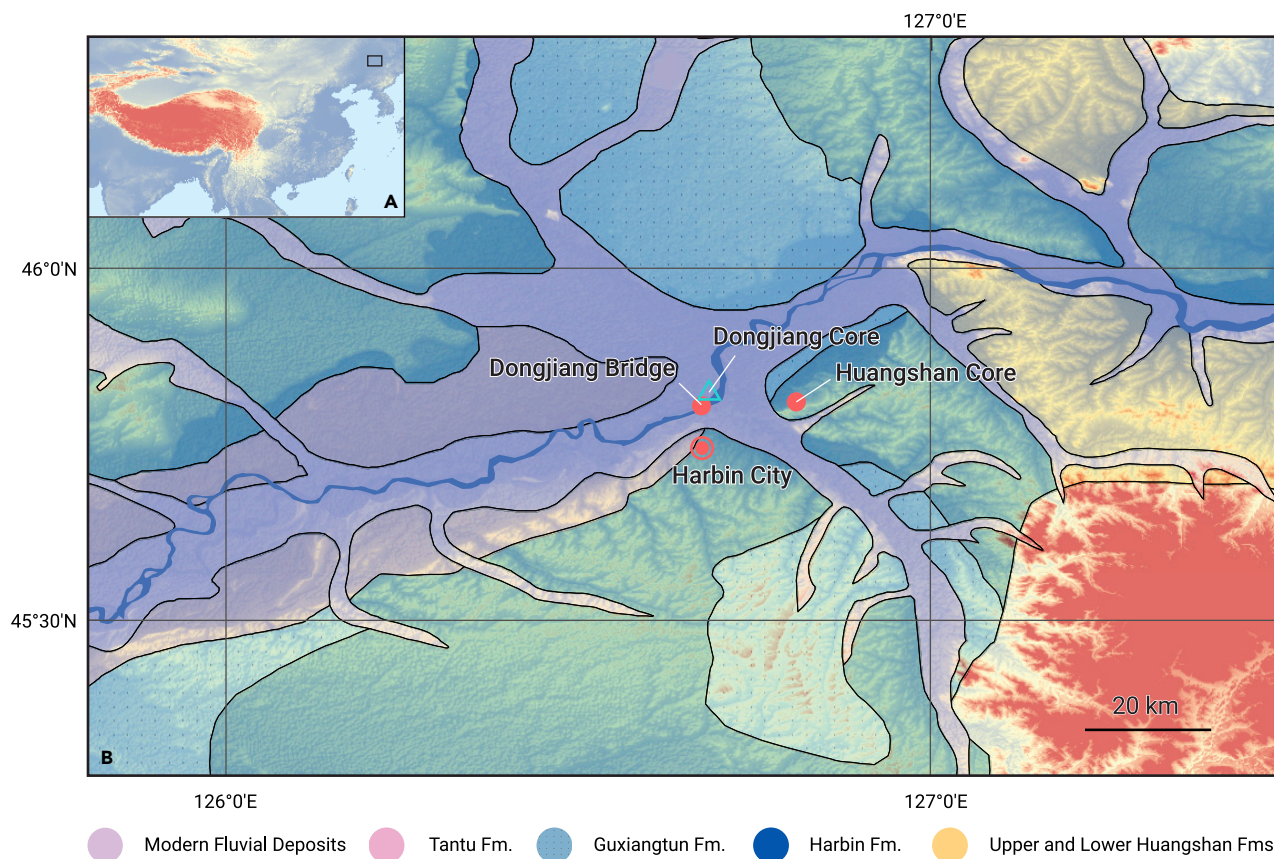


**Figure 1. The proposed location of the Harbin fossil cranium** (A) DEM image of China, with a rectangle indicating the study area. (B) Geological map of the Harbin area. Revised from the Wang and other workers.<sup>4–6</sup>

comparative specimens range from the Middle Pleistocene to Holocene, as indicated by their U-series apparent ages (Table S1).

The REE concentrations were determined using an HR-ICP-MS (high resolution inductively coupled plasma mass spectrometer). The REE results for the Harbin cranium and those for human/mammalian fossils with a common geographic origin for comparison are listed in Table S1, and shown as REE patterns normalized to PAAS (Post Archean Australian Shale) in a spider diagram in Figure 2B. Both the Harbin cranium and these analyzed fossils exhibit similar REE concentration patterns (Figure 2B). The light REE to heavy REE (LREE/HREE) ratio of the Harbin cranium is 3.668, following the range of these analyzed fossils (3.463–5.514). This range, including that of the Harbin cranium, is much lower than the LREE/HREE of PAAS (9.491), indicating that all these fossils show relatively low fractionation and HREE depletion. The total REE ( $\Sigma$ REE) value of the Harbin cranium is about 234.6  $\mu\text{g/g}$ , higher than those of the fossil specimens analyzed for comparison (with a range from 4.6 to 149.5  $\mu\text{g/g}$ ). The high  $\Sigma$ REE value of the Harbin cranium is probably due to its greater age, which results in longer and more complex diagenesis processes. The REE concentration patterns and the LREE/HREE values of the Harbin cranium and the Middle Pleistocene–Holocene human/mammalian fossils suggest that they probably have the same geographical origins.

### Strontium isotopic composition

Strontium (Sr) isotopic ratio is widely used as a petrogenetic tracer for determining the source of rock/sediment formations (e.g., Faure<sup>11</sup>). In anthropological and archeological researches, the technique is used to investigate prehistoric human migration,<sup>12–14</sup> ancient animal movements,<sup>15,16</sup> or special events of animal resources use.<sup>17</sup> Sr isotopic analyses were performed on the Harbin cranium ( $n = 1$ ), and the mammalian fossils ( $n = 7$ ) and human fossils ( $n = 2$ ) recovered from the deposits of the Songhua River

in the Harbin area, using an MC-ICPMS (multi-collector inductively coupled plasma mass spectrometer, Thermo Fisher Neptune). Moreover, the sediment samples adhering in the nasal cavity of the Harbin cranium ( $n = 1$ ) and from a core ( $n = 45$ ) drilled near the Dongjiang Bridge (DJ core, Figure 1B) were also analyzed.

The  $^{87}\text{Sr}/^{86}\text{Sr}$  ratio of the Harbin cranium shows a value of  $0.709423 \pm 0.000009$ , comparable with that of the analyzed human/mammalian fossils, ranging from 0.709066 to 0.709574 (Table S2; Figure 3). The Sr isotopic ratios of these fossils all fall in the variation range of the bioavailable Sr in the Harbin areas (0.7070–0.7110, Figure S3). The bioavailable Sr in the Harbin and the nearby areas has the lowest  $^{87}\text{Sr}/^{86}\text{Sr}$  ratios ( $<0.711$ ) in China (Figure S3), which is thought to be related to the mafic-ultramafic silicate rocks of the Xing'an-Mongolian orogenic belt.<sup>18</sup> These Sr isotopic data strongly suggest that they shared a common geological environment and bioavailable Sr source. The sediments adhered in the nasal cavity of the Harbin cranium consist of dark gray sandstone, most similar to those from the layer between 6.6 and 12.5 m of the DJ core. They yielded a  $^{87}\text{Sr}/^{86}\text{Sr}$  isotopic ratio of  $0.711898 \pm 0.000003$ , which falls in the variation ranges measured in the DJ core (from 0.709765 to 0.714884) and is close to the values of the sediments at the depths of  $\sim 12$  m of the DJ core (Figure 4).

### Lithostratigraphic correlation

The sedimentary sequence of the DJ core from the top to the unconformity with the Mesozoic includes nine layers (Figure 4). These layers are correlated with the Huangshan section (Figures 1 and 4), which is a standard section of the regional Quaternary stratigraphy, approximately 15 km from the DJ core.<sup>4</sup> The Huangshan section (HS section) and a core drilled at the Huangshan section (HS core) are well dated by magnetostratigraphic and optically stimulated luminescence (OSL) methods.<sup>4,5</sup> The HS core also has Sr isotopic ratios.<sup>5</sup> The second and third layers from top of the DJ core are

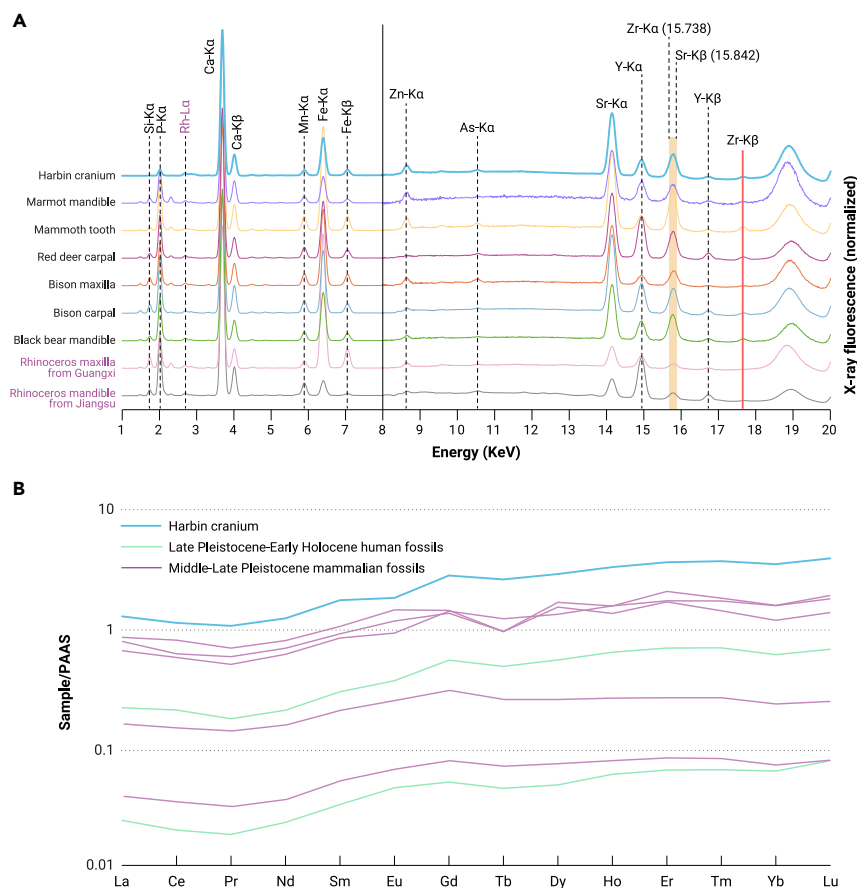


**Figure 2. Provenience analyses on the Harbin cranium and the fossil specimens analyzed for comparison (A) XRF element spectra. (B) REEs. Each XRF spectrum was normalized with the signal of the Rh-L $\alpha$  peak, which is generated by a Rh X-ray source. The rhinoceros maxilla and mandible from different sites were taken as control samples. The concentration patterns of the REEs were normalized by Post Archean Australian Shale (PAAS).**

set of yellowish-brown, alluvial fine muddy silt, alluvial silt, about 6.2 m thick. These two layers can be correlated to the Guxiangtun Formation/Harbin Formation of the HS section/HS core. The fourth to the sixth layers of the DJ core are characterized by gray to dark gray static water deposition of sludge-like mud and alluvial fine silt, about 5.9 m thick. These layers can be roughly correlated with the upper part of the Upper Huangshan Formation of the HS section/HS core, in which there are also more gray to dark gray muddy sediments than in other layers. The seventh and eighth layers of the DJ core include grayish-brown, fluvial sand and alluvial medium-grained sandy silt, about 29 m thick. The two layers should be correlated with the sandier lower

part of the Upper Huangshan Formation and the Lower Huangshan Formation of the HS section/HS core.

The Harbin area is one of the most fossiliferous areas in China. More than 70 species have been reported from this area.<sup>19–25</sup> Fossils collected from the deposits in the Songhua River near the Dongjiang Bridge are mainly from the upper yellowish-brown muddy silt layers (~Guxiangtun Formation/Harbin Formation), and the grayish mud and silt (~upper part of the Upper Huangshan Formation). The U-series dating on the fossil samples from seven mammals and two human individuals (Figures S1 and S2) yielded two groups of apparent

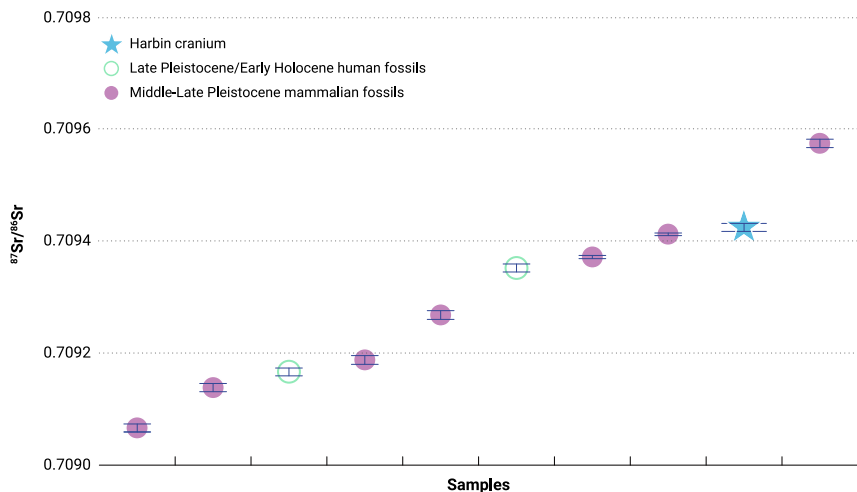


**Figure 3. Sr isotopic composition on the Harbin cranium and the Middle Pleistocene-Early Holocene mammalian and human fossils**



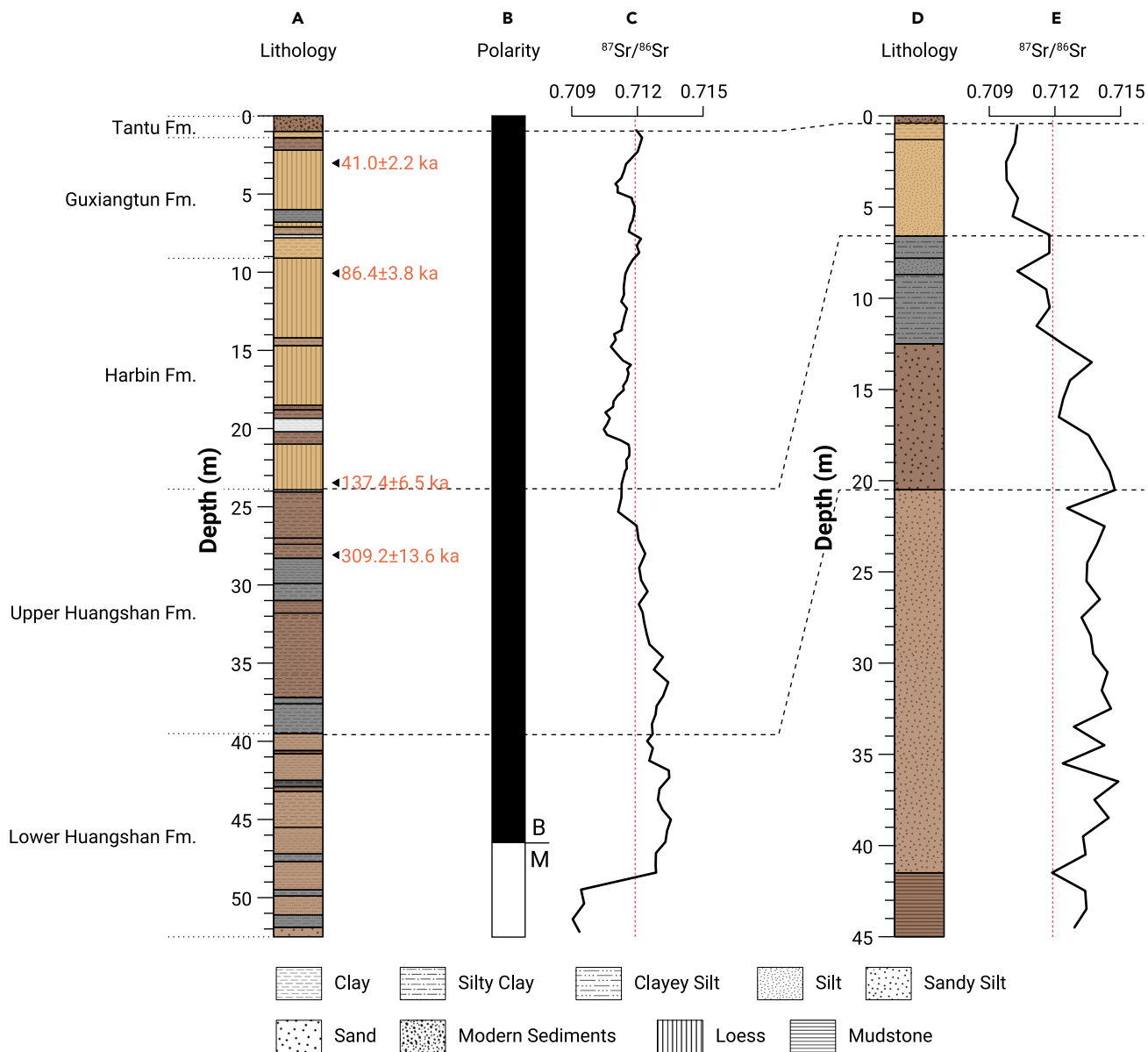


**Figure 4. Stratigraphic correlations and the Sr isotopic ratios of the sediments from the Huangshan section, Huangshan core, and Dongjiang core** (A and B) Lithostratigraphy and Paleomagnetic polarities from the Huangshan section, based on the data from Wang et al.<sup>4</sup> (C) Sr isotopic ratios from the Huangshan core, data from Wei et al.<sup>5</sup> (D and E) Lithostratigraphy and Sr isotopic ratios from the Dongjiang core, data are from this research. The Dongjiang Bridge core was drilled at 45°50'28"N, 126°36'27"E. The sedimentary sequence of the Dongjiang core from the top to the unconformity with the Mesozoic includes nine layers: (1) modern sediments, 0.4 m; (2) yellowish-brown, alluvial fine muddy silt, 0.9 m; (3) yellowish-brown alluvial silt, 5.3 m; (4) gray to dark gray, static water deposition, sludge-like mud, 1.2 m; (5) dark gray alluvial fine silt, 0.9 m; (6) dark gray, static water deposition, sludge-like mud, 3.8 m; (7) grayish-brown, fluvial sand, including ~3% of gravels, gravel diameter ~3 mm, 8 m; (8) grayish-brown alluvial medium grained sandy silt, 21 m; and (9) grayish-brown, mudstone, with parallel bedding, 3.5 m. The unconformity is between layer 8 and layer 9. The age in red is the OSL date. The red dashed lines indicate the Sr isotope ratio of the sediments adhering in the Harbin cranium.

ages, ranging from  $9 \pm 4$  to  $34.6 \pm 0.3$  ka, and from  $132.6 \pm 0.4$  to  $201 \pm 1$  ka (Table S3). The age of the Guxiangtun Formation/Harbin Formation is known as ~12–138 ka old, and the upper part of the Upper Huangshan Formation has an OSL dating constraints between 138 and 309 ka.<sup>4</sup> The two groups of direct U-series apparent ages of the mammalian/human fossils from the Harbin area fall in the age range of the two formations and are consistent with the stratigraphic correlations.

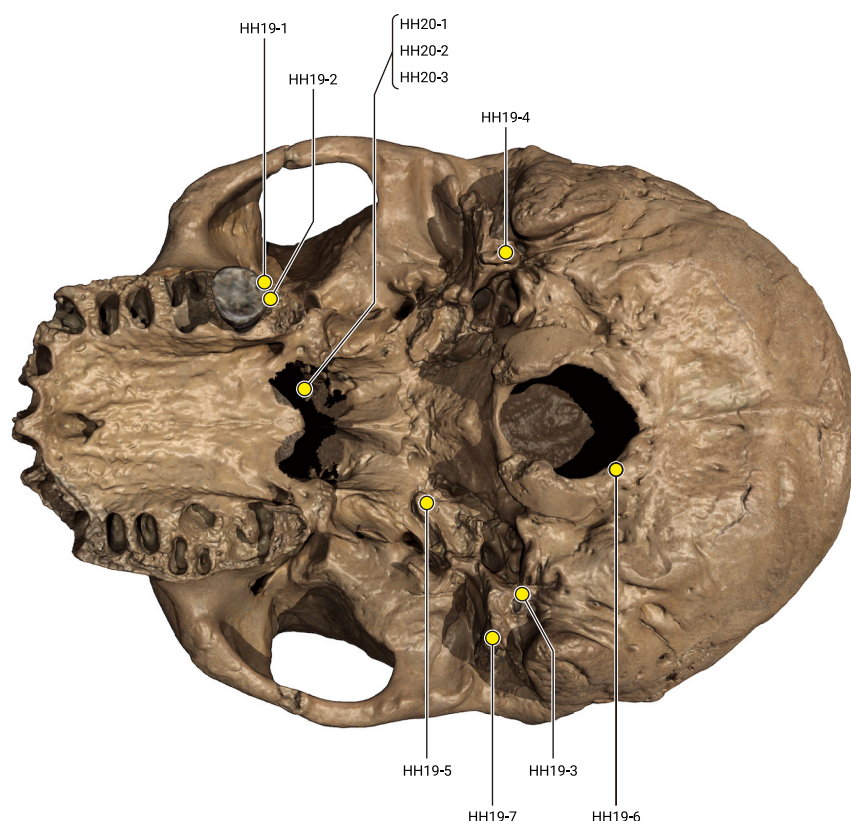
When the Sr isotopic ratios from the HS core<sup>5</sup> are compared with the DJ core (Figure 4), the fourth to sixth layers between 6.6 and 12.5 m of the DJ core show a similar gradual increase as the upper part of the Upper Huangshan Formation of the HS core at depths of ~30 m, which also yielded Sr isotopic ratios around 0.711898 (Figure 4). This result is also consistent with the stratigraphic correlations.

#### U-series dating

Owing to the poor provenance, we attempted to directly date this fossil cranium using a U-series method. Fossil bones are less desirable than carbonates for U-series dating, because fossil bones readily take up uranium from groundwater after deposition. However, if the incorporated uranium has not been leached out at some time after bone deposition, the U-series apparent age can provide the minimum age of the fossil.<sup>26</sup>

To minimize destruction on the Harbin fossil cranium, the samples ( $n = 10$ ) for U-series dating were hand drilled on the broken surfaces of the bones with 0.3 mm carbide-tipped drill bits, and the powdered sample size was kept between 0.1 and 0.5 mg (Figure 5). The U and Th isotopic measurements were performed on an MC-ICPMS (Thermo Fisher Neptune). The U-series dating results are summarized in Table S3. All samples lie within a narrow  $^{234}\text{U}/^{238}\text{U}$  activity ratio range (1.481–1.576), but show large variations in

**Figure 5. Sampling locations on the Harbin cranium for U-series dating analyses**



$^{230}\text{Th}/^{234}\text{U}$  activity ratio (0.474–1.039). The corrected U-series apparent ages are highly scattered, ranging from  $62 \pm 3$  to  $296 \pm 8$  ka, and the back-calculated initial  $^{234}\text{U}/^{238}\text{U}$  activity ratio ( $^{234}\text{U}/^{238}\text{U}$ ) ranged from 1.652 to 2.161 (Table S3).

The results can roughly be divided into two groups. The first group includes five samples that have relatively younger U-series apparent ages (from  $62 \pm 3$  to  $148 \pm 2$  ka), red data points in the isotope evolution diagram (Figure 6). Their isotopic data randomly scatter around the U-series evolution curve for an initial  $^{234}\text{U}/^{238}\text{U}$  of 1.70 (Figure 6). This pattern suggests that the source of uranium in these samples remained the same, but U-uptake took place over different time intervals without obvious evidence for post-burial U-leaching. The two youngest U-series apparent ages are  $62 \pm 3$  and  $85 \pm 4$  ka (HH19-1, 2), both obtained on the exposed dentine from the tooth roots of the surviving molar ( $M^2$ ). The young ages are probably caused by a delayed U-uptake, because the cementum and dentine of the tooth roots are much denser than the bones and probably obstructed uranium migration into the dentine. The other three U-series apparent ages,  $106 \pm 1$ ,  $129 \pm 1$ , and  $148 \pm 2$  ka, were obtained on HH19-6, 20-2, and 19-4, respectively. This group of data has no obvious evidence for U-leaching and is reasonable for estimating the minimum age of the Harbin cranium. The best minimum age estimate derived from this data group is the maximum value of the data group: that is  $148 \pm 2$  ka.

The second group (green data points in Figure 6) includes five samples with relatively older U-series apparent ages ( $185 \pm 2$  to  $296 \pm 8$  ka). This older age group shows higher  $^{230}\text{Th}/^{234}\text{U}$  isotope ratios and more widely scattered initial  $^{234}\text{U}/^{238}\text{U}$  ratios than the younger age group. It can be expected that, for a bone that experienced continuous U-uptake process, its  $^{230}\text{Th}/^{234}\text{U}$  activity ratio should be less than 1, but the occurrence of U-leaching can result in a shift of the  $^{230}\text{Th}/^{234}\text{U}$  activity ratio to higher values, even beyond isotopic equilibrium.<sup>27</sup> The subsample HH19-3 shows the oldest apparent U-series age of  $\sim 296$  ka, but it has  $^{230}\text{Th}$  activities in excess of  $^{234}\text{U}$  ( $^{230}\text{Th}/^{234}\text{U} = 1.031 \pm 0.006$ ), suggesting that this old age is very likely the result of U-leaching. The other four subsamples with older ages (HH19-5, 19-7, 20-1, and 20-3) have  $^{230}\text{Th}/^{234}\text{U}$  ratios close to isotopic equilibrium (0.943 on average), sug-

gesting that a slight U-leaching has occurred to these samples. Leached samples do not provide any useful age information, we therefore regard the age of 146 ka from the younger age group as the most conservative age (minimum age) estimate for the Harbin cranium.

The U-series apparent ages of the mammalian/human fossils from the Harbin area (Figures S1 and S2; Table S3) can be seen as the minimum ages of the corresponding fossil samples, except for the samples V23288 and F12, because their  $^{230}\text{Th}$  activities are in excess of  $^{234}\text{U}$ , and thus the occurrence of U-leaching cannot be excluded. All these samples show initial  $^{234}\text{U}/^{238}\text{U}$  (1.467–2.063) comparable with the values measured in the Harbin cranium (1.652–2.161), which provide another line of evidence that the Harbin cranium was probably from a similar burial environment as these fossils analyzed for comparison.

## DISCUSSION AND CONCLUSIONS

Our analyses reveal that the Harbin cranium has XRF element distribution patterns and REE concentration patterns like those of the mammalian and human fossils recovered from the Pleistocene sediments in the Harbin area. The  $^{87}\text{Sr}/^{86}\text{Sr}$  ratio of the Harbin cranium (0.709423) also falls in the range of these mammalian and human fossils for comparison (ranging from 0.709066 to 0.709574). All these  $^{87}\text{Sr}/^{86}\text{Sr}$  ratios are within the range of the regional bioavailable Sr isotope ratio values in the Harbin areas. The sediments adhered in the nasal cavity of the Harbin cranium show a  $^{87}\text{Sr}/^{86}\text{Sr}$  ratio of 0.711898, very close to the values measured at the upper part of the DJ core at a depth of  $\sim 12$  m. The regional stratigraphic correlations based on Sr isotopic data and lithostratigraphic characters indicate that the Harbin cranium probably was recovered from the upper part of the Upper Huangshan Formation. Direct U-series dating on the cranium ( $n = 10$ ) suggests that one group of the samples suffered U-leaching, and one group of the samples experienced continuous or delayed U-uptake without obvious evidence of U-leaching. The group without U-leaching yielded an apparent age of  $\sim 146$  ka as the most conservative age (minimum age) estimate for the Harbin cranium. This minimum age is consistent with the regional stratigraphic correlation. While the multiple lines of evidence from

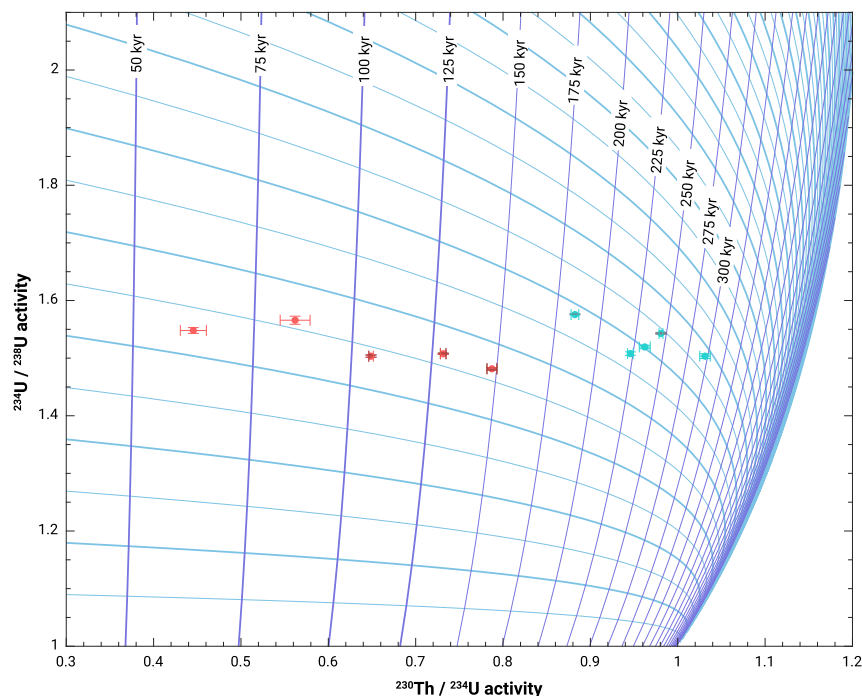


**Figure 6. U-series evolution diagram showing the activity ratios observed on the Harbin cranium** Light blue lines show U-series evolution in closed-system for selected initial  $^{234}\text{U}/^{238}\text{U}$  values. Red data points randomly scattered around the evolution curve with initial  $^{234}\text{U}/^{238}\text{U}$  of 1.70 are considered to be the results of U-uptake processes without the effect of U-leaching. Green data points are probably the results of U-uptake followed by U-leaching.

our experiments cannot pin the Harbin cranium to an exact site and layer, they consistently support the conclusion that this human specimen is from the late Middle Pleistocene of the Harbin area.

The late Middle Pleistocene Harbin archaic human (>146 ka) is roughly contemporaneous with some other Middle Pleistocene archaic humans from China, such as Xiahe ( $\geq 160$  ka),<sup>28</sup> Jinniushan ( $\geq 200$  ka),<sup>29</sup> Dali (327–240 ka),<sup>30,31</sup> and Hualongdong (345–265 ka).<sup>32</sup> This age span also overlaps with the early *H. sapiens* from Africa and the Mideast. If these East Asian archaic humans indeed belong to a monophyletic evolutionary lineage sister to the *H. sapiens* lineage,<sup>1</sup> this human lineage must have been as successful as the early *H. sapiens* populations in Africa and the Mideast, because they distributed in a very large area, including some extreme environments (high altitude and high latitude).

## MATERIAL AND METHODS

### Provenance test

We used non-destructive XRF analyses, following the procedures of Li et al.,<sup>33</sup> to examine the element distribution of the Harbin cranium and a range of mammalian fossils ( $n = 6$ ) collected from submerged sediments near the Dongjiang Bridge (Figure 1). The mammalian fossils are Middle-Late Pleistocene in age. Two mammalian fossils from sites in southern China were used as control samples. All the fossil specimens are under the oversight of the institutional review board of the Hebei GEO University or the Institute of Vertebrate Paleontology and Paleoanthropology. XRF analyses were performed on the M4 TORADO PLUS Micro-SRF analyzer at the Institute of Geology and Geophysics, Chinese Academy of Sciences. One area of about  $\sim 1\text{--}2$  cm<sup>2</sup> for each sample was randomly selected for collecting the XRF signals. Measuring parameters were set at 50 kV of high voltage and 40  $\mu\text{m}$  of pixel size. For semi-quantitative comparisons, each XRF spectrum was normalized with the signal of the Rh-L $\alpha$  peak, which is generated by a Rh X-ray source.

Small bone pieces ( $\sim 100$  mg) from the nasal cavity of the Harbin cranium were carefully collected for REE and Sr isotopic analyses. For comparison, fossil fragments from mammals (Figure S1,  $n = 6$ ) and late Pleistocene-Holocene human individuals (Figures S2 and S3,  $n = 2$ ) recovered from the Dongjiang Bridge area were analyzed. The sediment samples adhering in the nasal cavity of the Harbin cranium ( $n = 1$ ) and from a core ( $n = 45$ ) drilled near the Dongjiang Bridge were also used for Sr isotopic analyses.

REE analyses were performed at the State Key Laboratory for Mineral Deposits Research, Nanjing University. A Thermo Fisher Element XR HR-ICP-MS was used for the REE analyses. The samples were processed using the method in Trueman et al.<sup>34</sup> The rhodium solution (10 ppb) was dropped into the sample solutions for instrument drift correction. Analytical precision was <5% for each

element. An MC-ICPMS (multiple collector inductively coupled plasma mass spectrometer, Thermo Fisher Neptune) in Nanjing Normal University was used for the Sr isotopic analyses. Sample preparation and measurement methods followed that of Lei et al.<sup>35</sup> The measured  $^{87}\text{Sr}/^{86}\text{Sr}$  ratio was corrected for mass fractionation by normalization to a constant  $^{86}\text{Sr}/^{88}\text{Sr}$  ratio of 0.1194 using an exponential law. The isobaric interference of  $^{87}\text{Rb}$  on  $^{87}\text{Sr}$  was corrected using a natural  $^{87}\text{Rb}/^{85}\text{Rb}$  ratio of 0.3857. Replicate measurements of the NIST SRM 987 standard yielded a mean value of  $^{87}\text{Sr}/^{86}\text{Sr} = 0.710263 \pm 0.000014$  ( $2\sigma$ ,  $n = 11$ ) during the analytical period.

### U-series analysis

We carried out the U-series analysis directly on the Harbin cranium. Sample preparation followed that of Shao et al.<sup>36</sup> The U and Th isotopic measurements were performed on an MC-ICPMS (Thermo Fisher Neptune) in Nanjing Normal University. It is equipped with nine Faraday cups and a secondary electron multiplier (SEM). A retarding potential quadrupole energy filter was positioned in front of the SEM. An Aridus-II desolvator system (Cetac) couple with an ESI-50 nebulizer and an AutoSampler (ASX-520) was used for sample introduction. The U-series analysis results are summarized in Table S3. The isotopic variation and age distribution indicate that the U-uptake histories are heterogeneous in the Harbin cranium. A group of samples showing no evidence of U-leaching<sup>26</sup> had a U-series apparent age range of  $62 \pm 3$  to  $148 \pm 2$  ka. We consider that the oldest U-series apparent age ( $148 \pm 2$  ka) is a minimum age estimate for the Harbin cranium.

## REFERENCES

- Ni, X., Ji, Q., Wu, W., et al. (2021). Massive cranium from Harbin establishes a new Middle Pleistocene human lineage in China. *The Innovation* 2, 100130. In this issue. <https://doi.org/10.1016/j.xinn.2021.100130>.
- Ji, Q., Wu, W., Ji, Y., et al. (2021). Late Middle Pleistocene Harbin cranium represent a new *Homo* species. *The Innovation* 2, 100132. In this issue. <https://doi.org/10.1016/j.xinn.2021.100132>.
- Ji, Q., Ji, Y., Wang, X., et al. (2018). Discovery of *Homo heidelbergensis*-like skull fossil in Northeast China. *J. Geol.* 42, 349–350.
- Wang, Y., Dong, J., and Yang, J. (2020). Quaternary stratigraphy of the Huangshan section in Harbin. *Eur. Sci.* 45, 2662–2672.
- Wei, Z., Xie, Y., Kang, C., et al. (2020). The inversion of the Songhua River system in the early Pleistocene: implications from Sr-Nd isotopic composition in the Harbin Huangshan cores. *Act. Sedimentol. Sin.* 38, 1192–1203. <https://doi.org/10.14027/j.issn.1000-0550.2019.112>.
- Bureau of Geology and Mineral Resources of Heilongjiang Province (BGMHRP). (1993). *Regional Geology of Heilongjiang Province*. People's Republic of China, Ministry of Geology and Mineral Resources (Geological Memoirs (Geological Publishing House), p. 734.

7. Grandstaff, D.E., and Terry, D.O. (2009). Rare earth element composition of Paleogene vertebrate fossils from Toadstool Geologic Park, Nebraska, USA. *Appl. Geochem.* **24**, 733–745. <https://doi.org/10.1016/j.apgeochem.2008.12.027>.
8. Dalton, R. (2009). Elements reveal fossils' origins. *Nature* **459**, 309. <https://doi.org/10.1038/459307a>.
9. Suarez, C.A., Macpherson, G.L., González, L.A., et al. (2010). Heterogeneous rare earth element (REE) patterns and concentrations in a fossil bone: implications for the use of REE in vertebrate taphonomy and fossilization history. *Geochim. Cosmochim. Acta.* **74**, 2970–2988. <https://doi.org/10.1016/j.gca.2010.02.023>.
10. Herwartz, D., Tütken, T., Jochum, K.P., et al. (2013). Rare earth element systematics of fossil bone revealed by LA-ICPMS analysis. *Geochim. Cosmochim. Acta.* **103**, 161–183. <https://doi.org/10.1016/j.gca.2012.10.038>.
11. Faure, G. (1977). *Principles of Isotope Geology* (John Wiley and Sons, Inc.), p. 464.
12. Richards, M., Harvati, K., Grimes, V., et al. (2008). Strontium isotope evidence of Neanderthal mobility at the site of Lakonis, Greece using laser-ablation PIMMS. *J. Archaeol. Sci.* **35**, 1251–1256. <https://doi.org/10.1016/j.jas.2007.08.018>.
13. Copeland, S.R., Sponheimer, M., de Ruiter, D.J., et al. (2011). Strontium isotope evidence for landscape use by early hominins. *Nature* **474**, 76–78. <https://doi.org/10.1038/nature10149>.
14. Lugli, F., Cipriani, A., Capocchi, G., et al. (2019). Strontium and stable isotope evidence of human mobility strategies across the Last Glacial Maximum in southern Italy. *Nat. Ecol. Evol.* **3**, 905–911. <https://doi.org/10.1038/s41559-019-0900-8>.
15. Balasse, M., Smith, A.B., Ambrose, S.H., et al. (2003). Determining sheep birth seasonality by analysis of tooth enamel oxygen isotope ratios: the Late Stone Age site of Kasteelberg (South Africa). *J. Archaeol. Sci.* **30**, 205–215. <https://doi.org/10.1006/jasc.2002.0833>.
16. Britton, K., Grimes, V., Niven, L., et al. (2011). Strontium isotope evidence for migration in late Pleistocene Rangifer: implications for Neanderthal hunting strategies at the Middle Palaeolithic site of Jonzac, France. *J. Hum. Evol.* **61**, 176–185. <https://doi.org/10.1016/j.jhevol.2011.03.004>.
17. Madgwick, R., Lamb, A.L., Sloane, H., et al. (2019). Multi-isotope analysis reveals that feasts in the Stonehenge environs and across Wessex drew people and animals from throughout Britain. *Sci. Adv.* **5**, eaau6078. <https://doi.org/10.1126/sciadv.aau6078>.
18. Wang, X., and Tang, Z. (2020). The first large-scale bioavailable Sr isotope map of China and its implication for provenance studies. *Earth Sci. Rev.* **210**, 103353. <https://doi.org/10.1016/j.earscirev.2020.103353>.
19. Institute of Vertebrate Paleontology CAS. (1959). *Pleistocene Mammalian Fossils from the Northeastern Provinces* (Science Press), p. 82.
20. Zhengyi, W. (1973). The Quaternary mammalian fossils discovered in the Heilongjiang Province. *Chin. Sci. Bull.* **18**, 38–40.
21. Cai, B., and Yin, J. (1992). Late Pleistocene fossil mammals from Qinggang, Heilongjiang Province. *Bull. Chin. Acad. Geol. Sci.* **25**, 131–138.
22. Huili, Y., and Wei, D. (2011). Pleistocene mammalian fauna from the Jiaojie Cave at Acheng, Heilongjiang Province. *Quat. Sci.* **31**, 675–688.
23. Yang, Y., Li, Q., Fostowicz-Freluk, L., et al. (2019). Last record of *Trogontherium cuvieri* (Mammalia, Rodentia) from the late Pleistocene of China. *Quat. Int.* **513**, 30–36. <https://doi.org/10.1016/j.quaint.2019.01.025>.
24. Ni, X., Li, Q., Stidham, T.A., et al. (2020). Earliest-known intentionally deformed human cranium from Asia. *Archaeol. Anthropol. Sci.* **12**, 93. <https://doi.org/10.1007/s12520-020-01045-x>.
25. Lu, D., Yang, Y., Li, Q., et al. (2020). A late Pleistocene fossil from Northeastern China is the first record of the dire wolf (Carnivora: *Canis dirus*) in Eurasia. *Quat. Int.* **591**, 87–92. <https://doi.org/10.1016/j.quaint.2020.09.054>.
26. Grün, R., Eggins, S., Kinsley, L., et al. (2014). Laser ablation U-series analysis of fossil bones and teeth. *Palaeogeogr. Palaeoclimatol. Palaeoecol.* **416**, 150–167. <https://doi.org/10.1016/j.palaeo.2014.07.023>.
27. Duval, M., Aubert, M., Hellstrom, J., et al. (2011). High resolution LA-ICP-MS mapping of U and Th isotopes in an early Pleistocene equid tooth from Fuente Nueva-3 (Orce, Andalusia, Spain). *Quat. Geochronol.* **6**, 458–467. <https://doi.org/10.1016/j.quageo.2011.04.002>.
28. Chen, F., Welker, F., Shen, C.-C., et al. (2019). A late Middle Pleistocene Denisovan mandible from the Tibetan plateau. *Nature* **569**, 409–412. <https://doi.org/10.1038/s41586-019-1139-x>.
29. Lu, Z., Meldrum, D.J., Huang, Y., et al. (2011). The Jinniushan hominin pedal skeleton from the late Middle Pleistocene of China. *Homo* **62**, 389–401. <https://doi.org/10.1016/j.jchb.2011.08.008>.
30. Wu, X. (2020). Middle Pleistocene human skull from Dali, China. *Palaeont. Sin. N. Ser. D* **13**, 1–205.
31. Wu, X., and Athreya, S. (2013). A description of the geological context, discrete traits, and linear morphometrics of the Middle Pleistocene hominin from Dali, Shaanxi Province, China. *Am. J. Phys. Anthropol.* **150**, 141–157.
32. Wu, X.-J., Pei, S.-W., and Cai, Y.-J. (2019). Archaic human remains from Hualongdong, China, and Middle Pleistocene human continuity and variation. *Proc. Natl. Acad. Sci. U S A* **116**, 9820–9824. <https://doi.org/10.1073/pnas.1902396116>.
33. Li, J., Pei, R., Teng, F., et al. (2021). Micro-XRF study of the troodontid dinosaur Jianianhualong tengi reveals new biological and taphonomical signals. *Atom. Spectrosc.* **42**, 1–11.
34. Trueman, C.N., Behrensmeier, A.K., Potts, R., et al. (2006). High-resolution records of location and stratigraphic provenance from the rare earth element composition of fossil bones. *Geochim. Cosmochim. Acta.* **70**, 4343–4355. <https://doi.org/10.1016/j.gca.2006.06.1556>.
35. Lei, H.-L., Yang, T., Jiang, S.-Y., et al. (2019). A simple two-stage column chromatographic separation scheme for strontium, lead, neodymium and hafnium isotope analyses in geological samples by thermal ionization mass spectrometry or multi-collector inductively coupled plasma mass spectrometry. *J. Sep. Sci.* **42**, 3261–3275. <https://doi.org/10.1002/jssc.201900579>.
36. Shao, Q.-F., Li, C.-H., Huang, M.-J., et al. (2019). Interactive programs of MC-ICPMS data processing for <sup>230</sup>Th/U geochronology. *Quat. Geochronol.* **51**, 43–52. <https://doi.org/10.1016/j.quageo.2019.01.004>.

#### ACKNOWLEDGMENTS

We thank colleagues of the Heilongjiang Academy of Geological Sciences who helped with core drilling and sample collections. Drs. T. Yang and H.-L. Lei from the Nanjing University helped with the REE and Sr isotopic analyses. Dr. Z. Tang provided the recent published bioavailable Sr isotopic mapping data. We are grateful for the support of Drs. F. Wang, C. Li, X. Wu, D. Zhang, L. Crété, and T. Deng, as well as R. Tang for his help on making the figures. We thank Dr. Y.-Y. Xie from the Harbin Normal University for providing the Sr isotope ratio data of the Huangshan core. This project has been supported by the National Natural Science Foundation of China (41977380, 41877430, 41842039, 41625005, 41888101, 41988101), the Strategic Priority Research Program of Chinese Academy of Sciences (CAS XDB26030400, XDB26030300, XDA20070203, XDA19050100), the People's Government of Hebei Province (Z20177187), the China Geological Survey (DD20190601), the Science Foundation of Hebei GEO University (TS2017-001), and the Second Tibetan Plateau Scientific Expedition and Research Program (2019QZKK0705). C.S.'s research is supported by the Calleva Foundation and the Human Origins Research Fund. We thank the reviewers for their help in improving the article.

#### AUTHOR CONTRIBUTIONS

Q.J. obtained the Harbin cranium and organized the project. Q.S. performed U-series dating, REE and Sr isotopic analyses, analyzed the U-series dating data, and wrote the manuscript. J.G. analyzed the REE and Sr isotopic data, and wrote the manuscript. J.L. performed XRF analyses, and edited the manuscript. R.G. analyzed the U-series dating data, and edited the manuscript. Q.L. collected the mammalian fossils, and edited the manuscript. W.W., Y.J., and T.Z. collected data, drilled the core, and measured sections. C.S. and C.Z. edited the manuscript. X.N. analyzed the data, organized the project, and wrote the manuscript.

#### DECLARATION OF INTERESTS

The authors declare no competing interests.

#### SUPPLEMENTAL INFORMATION

Supplemental information can be found online at <https://doi.org/10.1016/j.xinn.2021.100131>.